HHS Public Access

Author manuscript

Neuroimage. Author manuscript; available in PMC 2018 January 15.

Published in final edited form as:

Neuroimage. 2017 January 15; 145(Pt B): 265–273. doi:10.1016/j.neuroimage.2015.12.013.

Machine Learning of Structural Magnetic Resonance Imaging Predicts Psychopathic Traits in Adolescent Offenders

Vaughn R. Steele[1,2,3,*], **Vikram Rao**[2], **Vince D. Calhoun**[2,4,5,6], and **Kent A. Kiehl**[2,3,6,*]

[1]Intramural Research Program, Neuroimaging Research Branch, National Institute of Drug Abuse, National Institutes of Health, Baltimore, MD, USA

[2]The nonprofit Mind Research Network (MRN) & Lovelace Biomedical and Environmental Research Institute (LBERI), Albuquerque, NM, USA

[3]Department of Psychology, University of New Mexico, Albuquerque, NM, USA

[4]Department of Electrical and Computer Engineering, University of New Mexico, Albuquerque, NM, USA

[5]Department of Psychiatry, University of New Mexico, Albuquerque, NM, USA

[6]Department of Neurosciences, University of New Mexico, Albuquerque, NM, USA

Abstract

Classification models are becoming useful tools for finding patterns in neuroimaging data sets that are not observable to the naked eye. Many of these models are applied to discriminating clinical groups such as schizophrenic patients from healthy controls or from patients with bipolar disorder. A more nuanced model might be to discriminate between levels of personality traits. Here, as a proof-of-concept, we take an initial step toward developing prediction models to differentiate individuals based on a personality disorder: psychopathy. We included three groups of adolescent participants: incarcerated youth with elevated psychopathic traits (i.e., callous and unemotional traits and conduct disordered traits; $n = 71$), incarcerated youth with low psychopathic traits ($n = 72$), and non-incarcerated youth as healthy controls ($n = 21$). Support vector machine (SVM) learning models were developed to separate these groups using an out-of-sample cross-validation method on voxel-based morphometry (VBM) data. Regions-of-interest from the paralimbic system, identified in an independent forensic sample, were successful in differentiating youth groups. Models seeking to classify incarcerated individuals to have high or low psychopathic traits achieved 69.23% overall accuracy. As expected, accuracy increased in models differentiating healthy controls from individuals with high psychopathic traits (82.61%) and low psychopathic traits (80.65%). Here we have laid the foundation for using neural correlates of personality traits to identify group membership within and beyond psychopathy. This is only the first step, of many,

[*]**Corresponding authors:** Vaughn R. Steele, Ph.D., National Institute on Drug Abuse, National Institutes of Health, 251 Bayview Blvd, Baltimore, MD 21224, vaughn.r.steele@gmail.com, Kent A. Kiehl, Ph.D., The Mind Research Network, 1101 Yale Blvd NE, Albuquerque, NM, 87106, kkiehl@mrn.org.

toward prediction models using neural measures as a proxy for personality traits. As these methods are improved, prediction models with neural measures of personality traits could have far-reaching impact on diagnosis, treatment, and prediction of future behavior.

Keywords

prediction; voxel-based morphometry; SVM; psychopathy

1.0 Introduction

Finding patterns in large and sometimes noisy datasets with classification models has become more common. Internet search engines, facial recognition software, and exploring big data are all examples of classification models used to identify patterns in data. As these models become more and more accurate, researchers seek to develop models predicting a specific outcome for a single participant. Considering the complexity and difficult nature of such an endeavor, it may take years for science to develop the theoretically possible highly accurate prediction models of a single participant. Prediction at the level of an individual may be most useful in a few areas with heterogeneous and co-morbid clinical diagnoses. Here we take an initial step toward fine-tuning prediction models with the purpose of affecting positive, individual outcomes.

As several classification models have become more and more prevalent, accuracy in distinguishing groups of individuals has increased. Models discriminating healthy subjects from patients with severe mental illnesses have demonstrated promise, including schizophrenia (Arbabshirani et al., 2013; Schnack et al., 2014; Silva et al., 2014; Sui et al., 2009; Yang et al., 2010a), bipolar disorder (Schnack et al., 2014), psychosis (Arribas et al., 2010; Calhoun et al., 2008; Sun et al., 2009), and Huntington's Disease (Rizk-Jackson et al., 2011). Also, models have been used to predict brain maturation (Dosenbach et al., 2010), substance use (Fan et al., 2006; Pariyadath et al., 2014; Zhang et al., 2005), and substance use outcomes (Marhe et al., 2013; Steele et al., 2014). Clinical diagnosis such as depression (Habes et al., 2013) and obsessive compulsive symptoms (Weygandt et al., 2012a; Weygandt et al., 2012b) have also been successfully differentiated with prediction models. Each of these prediction models were designed to reduce subjectivity in distinguishing groups by including neuroimaging, genetics, and/or clinical assessment data. In many cases, these models are developed to distinguish between groups that are quite different from each other. A more nuanced discrimination between individuals would be to distinguish individuals on their severity of a specific personality trait or cluster of traits. This is challenging because personality traits often overlap with one another and with other comorbid conditions. Nevertheless, identifying neural correlates of a personality trait could prove more sensitive to differentiating individuals on that trait compared to using other proxy assessments, like self-report or expert-rater assessments.

A well-known and thoroughly examined personality trait is psychopathy, a serious personality disorder characterized by affective and behavioral symptoms. Just less than one percent of the general population is estimated to meet the established clinical criteria for

psychopathy, though the rate increases to 15-25% in incarcerated settings (Hare, 2003). Hare's Psychopathy Checklist-Revised (PCL-R; (Hare, 2003)) is the most common and validated instrument for assessing psychopathic traits in adult forensic settings. Identifying individuals with elevated psychopathic traits may be most beneficial in helping to assign treatments options that are effective (Caldwell, 2011; Caldwell et al., 2007) and not counterproductive (Rice and Harris, 1997). Psychopathic traits, known as callous and unemotional traits and conduct disordered traits (CU/CD) in youth, is most commonly assessed in juvenile forensic populations using the Hare Psychopath Checklist: Youth Version (PCL:YV (Forth et al., 2003), a downward extension of the adult Hare PCL-R. Research has shown that the PCL-YV identifies youth at the highest risk of committing serious and violent crimes as adolescents and/or adults (Davidson et al., 2000; Hawkins et al., 1998; Hawkins et al., 2000). Psychopathic traits, at least at low to moderate levels, detected early in life often decrease naturally (Frick et al., 2003; Lee et al., 2009; Lynam et al., 2007). However, for a subsample of youth with elevated psychopathic traits, the disorder appears to remain stable across development (Blonigen et al., 2006; Frick et al., 2003; Lynam et al., 2007; Obradovic et al., 2007) and are referred to as being on the "life-course persistent" trajectory (Moffitt, 1993). Identifying risk factors specific to individuals with a life-course persistent trajectory could become useful when assigning treatment or potential long-term risk.

Individuals with elevated psychopathic traits, young and old, have exhibited cognitive and structural deficits originating in paralimbic areas (Kiehl, 2006). A growing body of literature supports this paralimbic hypothesis suggesting individuals with elevated psychopathic traits exhibit aberrant structure (specifically reduced grey matter volume and density) and function in many regions: anterior cingulate cortex (ACC), bilateral amygdala, bilateral hippocampus, medial orbitofrontal cortex (mOFC), bilateral orbitofrontal cortex (OFC), bilateral parahippocampus, posterior cingulate cortex (PCC), & bilateral temporal pole (Figure 1). Adults and youth with elevated psychopathic traits exhibit similar paralimbic neural dysfunction (Blair, 2006; Budhani and Blair, 2005; Cope et al., 2014; Ermer et al., 2012; Ermer et al., 2013; Harenski et al., 2014; Kiehl, 2006; Lockwood et al., 2013; Marsh et al., 2008; Motzkin et al., 2011; Raine et al., 2003). Deficits appear to be specific to the orbitofrontal cortex (Budhani and Blair, 2005; Cope et al., 2014; Ermer et al., 2013), insula (Lockwood et al., 2013), amygdala (Harenski et al., 2014; Marsh et al., 2008), PCC (Ermer et al., 2013), parahippocampal gyrus (Ermer et al., 2013), and ACC (Cope et al., 2014; Ermer et al., 2013; Marsh et al., 2008).

Well-established structural differences have been identified between adults and youth with and without elevated psychopathic or CU/CD traits. A combination of these structural differences may prove more sensitive to differentiating individuals with and without elevated psychopathic traits than other measures. Therefore, as a proof-of-concept, we develop prediction models with well-established a-priori regions of interest (ROI) of structural data alone to identify levels of psychopathic traits by comparing incarcerated individuals with elevated psychopathic traits, incarcerated individuals with low psychopathic traits, and healthy controls. If successful, a framework will be established to identify neural correlates of many personality traits. Potentially, neural measures of personality traits could yield

precise measures of the trait and therefore be practically useful in assessing that trait at an individual level.

Support vector machine (SVM) learning models are developed to separate groups with an out-of-sample cross-validation method. In these models, we use voxel-based morphometry (VBM) data extracted from paralimbic regions of interest (Ermer et al., 2013; Kiehl, 2006) known to be aberrant in individuals with elevated psychopathic traits. It is hypothesized prediction models will be able to differentiate groups using only the VBM ROIs. Once there is evidence that simple VBM ROI analyses are sufficient to separate groups, more sophisticated methods will be employed to refine future prediction models. Predicting levels of psychopathic traits in an individual with precision could have far-reaching impact on diagnosis of other personality traits, treatment, and potential future behavior.

2.0 Methods

2.1 Participants

These data were drawn from the National Institute of Mental Health (NIMH)-funded SouthWest Advanced Neuroimaging Cohort, Youth Sample (SWANC-Y), collected between June, 2007, and March, 2011, from ongoing research studies at a maximum-security youth detention facility in New Mexico. The present study reports on a subsample of these participants (all males; $n = 143$) for whom structural MRI and the Hare Psychopath Checklist: Youth Version (PCL: YV) (Forth et al., 2003) data were available (mean age = 17.29 years, standard deviation(SD) = 1.19). Using NIH racial and ethnic classification, 19% of the sample self-identified as White, 21% as Black/African American, 6% as American Indian, 36% as Other, 56% as Hispanic, 38% as not Hispanic, and 17% chose not to respond. The sample was primarily (89%) right handed. We selected individuals who scored at or above the clinical threshold of 30 on the PCL: YV ($n = 71$; mean = 32.78; SD = 2.23; range 30-38) and at or below 20 ($n = 72$; mean = 16.25; SD = 3.46; range 2-20). In addition, we report data from male healthy adolescent non-offender healthy controls drawn from the community ($n = 21$; mean age = 17.52 years, $SD = 2.53$). Using NIH racial and ethnic classification, 47.62% of the sample self-identified as White, 14.29% as Asian, 38.10% as Other, 38.10% as Hispanic, and 61.90% as not Hispanic. The healthy sample was primarily (91%) right handed.

This research was approved by the University of New Mexico Health Sciences Center Human Research Review Committee and all individuals volunteered to participate after providing written informed consent (if >= 18 years or age) or after providing written informed assent and parent/guardian written informed consent (if < 18 years of age). Participation did not affect institutional status (e.g., security level, privileges, parole, or release date). Individuals were excluded from participation if they had a history of seizures, epilepsy, psychosis, traumatic brain injury (TBI), other major medical problems, or failed to show fluency in English at or above a grade four reading level.

2.2 Assessments

Trained researchers administered assessments to each participant. These assessments included a measure of psychopathy (PCL: YV), intelligence quotient (IQ), and a TBI questionnaire. All offenders were assessed for psychopathy (i.e., callous and unemotional traits and impulsive/antisocial behaviors) using the expert-rater Psychopathy Checklist: Youth Version (Forth et al., 2003). The PCL: YV assessment includes a review of institutional records and a semi-structured interview that reviews individuals' school, family, work, and criminal histories, and their interpersonal and emotional skills. Individuals are scored on 20 items that measure personality traits and behaviors characteristic of psychopathy. Scores range from 0 to 40. The accepted diagnostic cutoff for psychopathy is 30 and above (Hare, 2003). Psychopathy includes interpersonal and affective traits, such as glibness, shallow affect, callousness, and lacking guilt and remorse (Factor 1) and lifestyle and antisocial traits, such as impulsivity, irresponsibility, and poor behavioral controls (Factor 2). The PCL: YV was not administered in the healthy sample.

Full-scale IQ was estimated from the Vocabulary and Matrix Reasoning subtests of the Wechsler Adult Intelligence Scale (Ryan et al., 1999; Wechsler, 1997) for participants older than 16 years of age and from the Wechsler Intelligence Scale for Children-Fourth Edition (Sattler and Dumont, 2004; Wechsler, 2003) for participants younger than 16 years of age. IQ estimates were unavailable for $n = 16$ incarcerated participants (mean = 90.02; SD = 13.40) and $n = 1$ for the healthy group (mean = 110.55; SD = 16.73). A post-head injury symptoms questionnaire (King et al., 1995) was administered to evaluate history of traumatic brain injury (TBI). No participant experience a TBI with significant loss of consciousness.

2.3 MRI Acquisition

High-resolution T1-weighted structural MRI scans were acquired on the Mind Research Network Siemens 1.5T Avanto mobile scanner, stationed at the detention facility (for offenders) or The Mind Research Network (for healthy controls), using a multi-echo MPRAGE pulse sequence (repetition time = 2530 ms, echo times = 1.64 ms, 3.50 ms, 5.36 ms, 7.22 ms, inversion time = 1100 ms, flip angle = 7°, slice thickness = 1.3 mm, matrix size = 256 × 256) yielding 128 sagittal slices with an in-plane resolution of 1.0 mm × 1.0 mm. Data were pre-processed and analyzed using Statistical Parametric Mapping software (SPM12; Wellcome Department of Cognitive Neurology, London, UK; http://www.fil.ion.ucl.ac.uk/spm) and VBM. T1 images were manually inspected by an operator blind to subject identity and realigned to ensure proper spatial normalization. Images were spatially normalized to the SPM12 T1 Montreal Neurological Institute (MNI) template, segmented into grey matter, white matter, and cerebrospinal fluid. Both volume and density were extracted for analyses. A Jacobian modulation was performed to preserve total volume (Ashburner and Friston, 2000, 2005). A nonlinear transformation without Jacobian determinants was performed on unmodulated images to extract grey matter density (Ashburner and Friston, 2000, 2005). Modulated and unmodulated images were resampled to 2 × 2 × 2 mm and smoothed with a 10 mm full-width at half-maximum (FWHM) Gaussian kernel. Voxels with a grey matter value of < 0.15 were excluded in order to remove possible edge effects between grey matter and white matter.

Thirteen regions of interest (ROI) were extracted to represent paralimbic regions using the AAL Wake Forest University Pick Atlas Toolbox in SPM12. Reduced grey matter in paralimbic regions have been shown in individuals with elevated psychopathic traits (Ermer et al., 2013; Kiehl, 2006). The thirteen regions include: ACC, bilateral amygdala, bilateral hippocampus, mOFC, bilateral OFC, bilateral parahippocampus, PCC, & bilateral temporal pole (Figure 1). Mean grey matter volume and density were extracted for each participant within each of these thirteen regions. These data were then used in predicting group membership (high scoring individuals, low scoring individuals, or healthy controls) in an out-of-sample cross-validated support vector machine learning classifier.

2.4 Support Vector Machine (SVM) Learning Classification

SVM were used to test nonlinear combinations of variables in identifying individuals as scoring high on the PCL: YV (30 and above), low on the PCL: YV (20 and below), or a healthy control. Measures of overall performance, sensitivity, and specificity were calculated for each SVM model. SVMs are especially beneficial when data classes are heterogeneous with few training samples (Melgani and Bruzzone, 2004). This binary classifier finds a hyperplane that maximizes the margin between two classes. Participants were classified using two nested leave-one-out cross-validations. Within each iteration, one participant is selected as the testing sample and the rest as training samples (first leave-one-out). To select the best parameter for the SVM classifier, a grid search was performed over parameters C and σ. C is the value of the box constraint for the soft margin and σ is the scaling factor of the radial basis function (RBF) kernel. Values for C were in this set [$C=2^{-2}$, $2^{-1.5}\ldots2^{6}$] and values for σ were in this set [$\sigma=2^{-2}$, $2^{-1.5}\ldots2^{4}$]. The classification rate was measured for each parameter set using another leave-one-out validation inside the training set. The best C and σ were identified by the model that produced the greatest combination of sensitivity and specificity. After selecting the best parameter, the left out testing sample was classified. Matlab version 7.12.0 (R2011a) was used to implement the svmtrain and svmclassify functions and a Gaussian RBF kernel to develop these classification models. Within each model, the variables were z-scored to standardize across the variable set. This procedure (using two nested leave-one-out) avoids any use of testing data in model selection or model training, which is crucial in any classification problem. This method has been used successfully with other datasets in our laboratory (Cope et al., 2014; Steele et al., 2015; Steele et al., 2014). There is a potential concern with over-fitting these models by included to many models with insufficient participants. Models differentiating healthy controls from incarcerated samples have the potential of over-fitting considering this is our smallest group with n = 21. Over-fitting may inflate accuracy in these models though this should not be a concern in the primary models of interest, classifying the two incarcerated samples which each include more than 70 participants.

Four support vector machine models were computed comparing each group: 1) Volume measures from 13 ROIs; 2) Density measures from 13 ROIs; 3) Volume and Density measures from 13 ROIs each; 4) age and IQ measure. For the first three models, grey matter volume and density were extracted for each participant within each of the 13 ROIs from paralimbic areas (Figure 1). These thirteen regions have been identified as being related to psychopathy (Kiehl, 2006), specifically an adolescent sample (Ermer et al., 2013) so as to

avoid biasing the classifier and artificially inflating the ability of brain regions to discriminate groups. Age and IQ measures were used in the final model. Accuracy of these models was confirmed with permutation tests. These tests were calculated by randomizing the labels (i.e., group membership as high or low PCL: YV or healthy control) 1000 times and calculating classification measures within each iteration. When randomizing the labels, the ratio of classes constant was held constant. By calculating the proportion of times (of the 1000 iterations) where the measures were greater than our original classification measures, *p*-values reflecting the stability of our classification models were calculated. The first three models comprehensively test whether structural volume and or density measures alone are sufficient in identifying high vs low scoring PCL: YV individuals. Additionally, these three models were used to identify high scoring PCL: YV individuals from healthy controls and low scoring PCL: YV individuals from healthy controls. The fourth model tests how well simple clinical measures perform in identifying group membership thus giving context to the relative performance of the first three models.

3.0 Results

3.1 High vs Low Scoring PCL: YV Individuals

Two-tailed *t*-tests were computed to test group differences in age and IQ. High scoring individuals (mean = 16.96, SD = 1.20) were slightly younger than low scoring individuals (mean = 17.62, SD = 1.09; $t(141) = 3.44$, $p < .001$). The two groups were not different on the IQ measures (high: mean = 88.41, SD = 14.36; low: mean = 91.67, SD = 12.26; $t(125) = 1.38$, $p = .172$). Supplemental Table 1 includes demographic information by group and comparisons among groups.

To evaluate nonlinear combinations of these variables predicting PCL: YV groups, four SVM models were computed (Table 1). Several of these models successfully predicted group membership at the individual level. Numerically, the best model using brain measures included both volume and density measures producing an overall accuracy of 69.23% (permutation generated *p*-value = .024). Importantly, this model successfully predicted participants in the high (70.42%) and low (68.06%) group relatively well. This was the best model overall outperforming the simpler model that included only age and IQ.

One-tailed *t*-tests examined whether less grey matter volume and density would be found in high scoring individuals compared to low scoring individuals (Table 2; See Supplemental Table 2 for mean and standard deviations for extracted volume and density measures). False discovery rate (FDR) corrections were applied and reported below (Benjamini and Hockberg, 1995; Yekutieli and Benjamini, 1997). Volume was significantly reduced in the high scoring group, relative to the low scoring group in the right temporal pole, $t(141) = 2.96$, $p = .026$.. Marginal reductions were also found in the right parahippocampus, $t(141) = 1.86$, $p = .074$, PCC, $t(141) = 2.09$, $p = .062$, left temporal pole, $t(141) = 2.34$, $p = .065$. Density measures did not differ between groups.

3.3 High Scoring PCL: YV Individuals vs Healthy Controls

Two-tailed *t*-tests were computed to test group differences in age and IQ. High scoring individuals (mean = 16.96, SD = 1.20) did not differ from the healthy controls (mean = 17.52, SD = 2.53; $t(90) = 1.41$, $p = .162$). IQ was significantly lower in the high scoring individuals (mean = 88.41, SD = 14.36) compared to the healthy controls (mean = 110.55, SD = 16.73; $t(82) = 5.78$, $p < .001$).

To evaluate nonlinear combinations of these variables predicting high scoring PCL: YV individuals and healthy controls, three SVM models were computed (Table 3). Several of these models successfully predicted group membership at the individual level. Numerically, the best model using brain measures included density measures and produced an overall accuracy of 82.61% (permutation generated *p*-value = .007). Importantly, this model successfully predicted participants in the low (83.10%) and healthy control (80.95%) group relatively well. The best model overall, was the fourth model that included only age and IQ, which produced an overall accuracy of 83.70% (permutation generated *p*-value = .003). Importantly, this model successfully predicted participants in the low (85.92%) and healthy control (76.19%) group better than the model that only included brain measures.

One-tailed *t*-tests were computed testing whether less grey matter volume and density would be measured in high scoring individuals compared to healthy controls (Table 2; See Supplemental Table 2 for mean and standard deviations for extracted volume and density measures). FDR corrections were applied and reported below (Benjamini and Hockberg, 1995; Yekutieli and Benjamini, 1997). Volume was significantly reduced in the high scoring group, relative to healthy controls, in all ROIs except the left amygdala, right parahippocampus, and PCC where it was marginally reduced. Density was significantly reduced in the high scoring group, relative to healthy controls, in all ROIs except the right hippocampus were it was marginally reduced.

3.3 Low Scoring PCL: YV Individuals vs Healthy Controls

Two-tailed *t*-tests were computed to test group differences in age and IQ. Similar ages were measured between low scoring individuals (mean = 17.62, SD = 1.09) and healthy controls (mean = 17.52, SD = 2.53; $t(91) = 0.27$, $p = .790$). IQ was significantly lower in the low scoring individuals (mean = 91.67, SD = 12.26) compared to the healthy controls (mean = 110.55, SD = 16.73; $t(81) = 5.47$, $p < .001$).

To evaluate nonlinear combinations of these variables predicting low scoring PCL: YV individuals and healthy controls, three SVM models were computed (Table 4). Several of these models successfully predicted group membership at the individual level. Numerically, the best model using brain measures included density measures and produced an overall accuracy of 80.65% (permutation generated *p*-value = .011). Importantly, this model successfully predicted participants in the low (83.33%) and healthy control (71.43%) group relatively well. The best model overall, was the fourth model that included only age and IQ, which produced an overall accuracy of 83.87% (permutation generated *p*-value = .004). Importantly, this model successfully predicted participants in the low (83.33%) and healthy control (85.71%) group better than the model that only included brain measures.

One-tailed *t*-tests were computed testing whether less grey matter volume and density would be measured in low scoring individuals compared to healthy controls (Table 2; See Supplemental Table 2 for mean and standard deviations for extracted volume and density measures). FDR corrections were applied and reported below (Benjamini and Hockberg, 1995; Yekutieli and Benjamini, 1997). Volume was significantly or marginally reduced in the low scoring group, relative to healthy controls, in all ROIs accept the left amygdala, right amygdala, left hippocampus, mOFC, left OFC, right parahippocampus, and PCC. Density was significantly or marginally reduced in the low scoring group, relative to healthy controls, in all ROIs accept the right hippocampus.

4.0 Discussion

Support vector machine (SVM) learning models were developed to separate groups of youth with and without elevated psychopathic traits and healthy controls. Groups were successfully differentiated using an out-of-sample cross-validation method and voxel-based morphometry (VBM) data extracted from paralimbic regions of interest (Ermer et al., 2013; Kiehl, 2006) previously shown to be aberrant in adults with elevated psychopathic traits. Predicting levels of personality traits in an individual with precision could have far-reaching impact on diagnosis, treatment, and prediction of future behavior. This proof-of-concept was successful in suggesting neural measures of personality traits, beyond psychopathy, could be used to differentiate groups of interest.

SVM prediction models differentiated high and low scoring PCL: YV individuals. The model with most stable predictions was one implementing grey matter volume measures (overall accuracy 69.23%; mean of all models = 67.02%, SD of all models = 2.78%). These SVM models highlight that although there were few significant volume and density measures between groups, prediction models were able to separate groups. These models should prove very useful in future attempts to delineate individuals with high or low levels of a personality trait using only structural measures. More research is warranted to generate better performing models considering the suggested threshold for clinically useful models is 80% accuracy (Savitz et al., 2013). The effects presented here are just below the 80% threshold; nonetheless, there is a promising future for experiments to obtain the proposed necessary accuracy.

As expected, SVM prediction models performed very well at distinguishing healthy controls from incarcerated individuals, regardless of psychopathic traits. These models were slightly more accurate in differentiating healthy controls from individuals with low psychopathic traits (overall accuracy 83.87%; mean of all models = 79.21%, SD of all models = 2.86%) than high psychopathic traits (overall accuracy 82.61%; mean of all models = 76.63%, SD of all models = 4.99%). In each case, however, the positive predictive value was relatively low. This is likely due to the unequal number of participants in each group considering only 21 healthy controls were available to compare to the incarcerated samples. It should also be noted that both incarcerated samples exhibited nearly universal reductions in grey matter and density relative to the healthy control sample. These differences proved to be relatively small numerically; however, suggesting the multivariate classifier used here may be most appropriate at differentiating groups with these small numerical differences. As such,

prediction models were successful in differentiating individuals with and without elevated psychopathic traits from healthy controls.

4.1 Potential Application

Models such as those developed here could have real-world application. For example, risk assessment in the legal system seeks to predict whether an individual will or will not re-offend. Subjective clinical predictions of future arrest have been shown to be highly inaccurate (Monahan, 1981). Subsequent research using empirically derived static (e.g., age, sex, criminal history) and dynamic (e.g., impulsivity, drug use, social support) risk factors have led to significant improvements in predicting future antisocial behavior (Douglas et al., 2002; Harris et al., 1993; Yang et al., 2010b). One of the strongest and most widely studied risk factors for recidivism is impulsivity or behavioral disinhibition (Harris et al., 1993; Yang et al., 2010b). Impulsivity, in this context, is defined as the persistent lack of restraint and consideration of future consequences (Harris et al., 1993). Recent work from our group has identified neural activity associated with the ACC and impulsivity to predicted subsequent rearrest better than behavioral variables (Aharoni et al., 2014; Aharoni et al., 2013; Steele et al., 2015). By combining all known risk factors, including structural, functional, and clinical assessment measures, risk assessment predictions may develop into precise measures at an individual level. Identifying individuals at greatest risk, especially at an early age, should provide the maximum benefit with recent development of targeted interventions (Caldwell, 2011; Caldwell et al., 2007). These interventions could augment the life-course persistent trajectory toward a more positive outcome. Also, adding neural measures to risk assessments could benefit the legal system by adding information and precision. This would allow judges to be more informed when making life-changing decisions for individuals in the criminal justice system. These decisions are currently being made with information identified to be useful in risk assessments such as gender, age, IQ, impulsivity, and psychopathic traits (Harris et al., 1993). Some argue our understanding of MRI is not sufficient for applications affecting decisions in the criminal justice system (c.f., lie detection (Rusconi and Mitchener-Nissen, 2013) though, as we have discussed previously (Aharoni et al., 2013; Steele et al., 2015), accurate predictions of future behavior of incarcerated individuals has proven elusive when relying on expert opinions and clinical assessments. Here, we suggest neural correlates of personality traits, structural measures (c.f. (Pardini et al., 2014)), and functional measures (c.f., (Aharoni et al., 2013; Steele et al., 2015)) could increase precision in legal risk assessment models while replication and extension of these findings is essential.

4.2 Limitations

A few limitations should be considered before applying what is described here to additional samples or individuals. First, we selected a few a-priori ROIs in our examination. Though these ROIs were selected based on areas known to be structurally or functionally aberrant in individuals with elevated psychopathic traits (Blair, 2006; Budhani and Blair, 2005; Cope et al., 2014; Ermer et al., 2012; Ermer et al., 2013; Harenski et al., 2014; Kiehl, 2006; Lockwood et al., 2013; Marsh et al., 2008; Motzkin et al., 2011; Raine et al., 2003), there could be additional ROIs that should be explored. Using data driven approaches, such as independent component analysis (ICA; (Calhoun et al., 2001; Caprihan et al., 2011; Xu et

al., 2009)) may prove to be more biologically valid, as we discuss in the future direction section below.

A second limitation is that the differences found between healthy controls and the individuals with and without elevated psychopathic traits may be due to something other than psychopathic traits. This is highlighted by the fact that the two incarcerated samples only differed on a few volume and density measures within ROIs; although, healthy controls and incarcerated samples were significantly different in many of the a-priori ROIs. The healthy controls were different in IQ and demographic characteristics from the two incarcerated samples. However, prediction models including only age and IQ measures were not as successful in differentiating individuals scoring high or low in psychopathy as models that included only brain measures. The greatest difference between groups is likely the levels of psychopathic traits considering most community samples score below 3 on the PCL-screening version. (Coid et al., 2009; Farrington, 2006; Neumann and Hare, 2008). Our community sample had no history of arrests, thus we are confident the community healthy control group all scored very low on psychopathic traits. Overall, it seems unlikely measures other than psychopathic traits were more influential in the prediction models. However, there is a potential for over-fitting of these models considering only n = 21 healthy controls were available for these classification models. Therefore, we suggest caution when interpreting or applying these two prediction models before replication.

Third, collecting and analyzing imaging data is likely more expensive than acquiring clinical assessment data. In the future it may be possible to develop neuro-prediction models that supplant classic risk instruments using structural MRI measures. Indeed, a single MRI scan could prove to be more cost effective than administering hours of clinical assessments. We present here a roadmap for predicting other personality traits toward a goal of replacing several clinical assessments with a single MRI scan.

A final limitation could be a lack of real-world application for the models developed here. As discussed above, this was a proof-of-concept that previously identified neural correlates of a personality trait could then be used to differentiate high and low scoring individuals in an independent sample. We have succeeded in the first step of this endeavor and the next few steps will be discussed below. Once a few additional steps are completed, we believe strong prediction models, at the level of the individual, will be possible.

4.3 Future Directions

Considering the models and results presented here, some intriguing future examinations are possible. Though the VBM measures of grey matter volume and density are often used, additional measures may yield more specific neural correlates useful in differentiating groups. Two methods in particular should be tested next. First, ICA of structural data (often referred to as source-based morphometry (SBM)) is a method to extract independent structures from the structural data (Calhoun et al., 2001; Caprihan et al., 2011; Xu et al., 2009). This method may be useful in identifying biologically valid structures that are both independent and useful in differentiating individuals on a spectrum within a specific personality trait. Second, FreeSurfer software suite (Dale et al., 1999); http://surfer.nmr.mgh.harvard.edu) is an automated atlas-based method of extracting volumetric

and cortical thickness measures using structural MRI data. FreeSurfer volumetric and cortical thickness measurements could be more representative of grey matter and therefore more sensitive to group differences. Future explorations using these more time-consuming and advanced methods beyond VBM could be useful in developing stronger prediction models than what is presented here.

More sophisticated analysis methods could be employed to better differentiate individuals on personality traits. The steps outlined here and using SBM or FreeSurfer to extract neural measures could help identify neural correlates of many personality traits in the future. As we have found previously, neural measure of error-processing and impulsivity are better predictors of future outcomes than the clinical assessment measures of impulsivity (Aharoni et al., 2013; Steele et al., 2015; Steele et al., 2014). This is highly suggestive neural correlates of personality trails could be validated to be as good, or better, at predicting future events than clinical assessments alone. Also, with the current analysis methodology, it is difficult to identify which variables are most useful in the classification. We interpret differences between groups in volume and density identified with *t*-tests to be most useful in the classification but it is likely that a combination of differences across variables is most useful in classification. Future analyses techniques could implement sophisticated methods to identify unique contributions from each variable toward classification to further out understanding on individual contributions.

Finally, the steps carried out here to differentiate individuals exhibiting high and low psychopathic traits could be applied to other personality traits. There are additional personality traits where differentiating clinical and subclinical levels could be beneficial. These benefits include accurately identifying which treatment (individual, group, or psychopharmacological) would be most effective, which individuals may benefit from treatment, which individuals pose the greatest risk to themselves or others, and potentially identifying an individual in need of treatment but does not necessarily meet current clinical cut-offs. By developing better models to be applied at the individual level, these, and many, other potential benefits are possible.

4.4 Conclusion

We have laid the foundation for using neural correlates of personality traits in identifying group membership for that personality trait. This proof-of-concept was possible with simple VBM measures and with more sophisticated measures (e.g., SBM and FreeSurfer) these models could be fine-tuned to capture groups more thoroughly. The models were applied here to psychopathy but could move beyond psychopathy to broaden the application of this type of prediction model. As highlighted here, many real-world applications of these models are possible. Primarily, neural correlates of personality traits may become valid predictors of future behavior and be used to assign individuals to specialized treatments. In each case, positive long-term outcomes would be expected at an individual level. This is only the first step, of many, toward prediction models using neural measures as a proxy for personality traits.

Supplementary Material

Refer to Web version on PubMed Central for supplementary material.

Acknowledgements

This study was funded by the National Institute of Mental Health (NIMH) grant 1R01MH071896 (K.A.K., PI), the National Institute of Biomedical Imaging and Bioengineering (NIBIB) grant 1R01EB006841 (V.D.C., PI) and the Eunice Kennedy Shriver National Institute of Child Health and Human Development (NICHD) grant 1R01HD082257 (K.A.K., PI). We thank Ebany Martinez-Finley, J. Michael Maurer, and Prashanth Nyalakanti for their contributions. We gratefully acknowledge the staff and inmates of the New Mexico Corrections Department, for without their generous cooperation this work could not have been completed.

6.0 References

Aharoni E, Mallett J, Vincent GM, Harenski CL, Calhoun VD, Sinnott-Armstrong W, Gazzaniga MS, Kiehl KA. Predictive accuracy in the neuroprediction of rearrest. Social neuroscience. 2014; 9:332–336. [PubMed: 24720689]

Aharoni E, Vincent GM, Harenski CL, Calhoun VD, Sinnott-Armstrong W, Gazzaniga MS, Kiehl KA. Neuro-prediction of future rearrest. Proceedings of the National Academy of Sciences of the United States of America. 2013; 110:6223–6228. [PubMed: 23536303]

Arbabshirani MR, Kiehl KA, Pearlson GD, Calhoun VD. Classification of schizophrenia patients based on resting-state functional network connectivity. Frontiers in neuroscience. 2013:7. [PubMed: 23378827]

Arribas JI, Calhoun VD, Adali T. Automatic Bayesian classification of healthy controls, bipolar disorder, and schizophrenia using intrinsic connectivity maps from FMRI data. IEEE transactions on bio-medical engineering. 2010; 57:2850–2860. [PubMed: 20876002]

Ashburner J, Friston KJ. Voxel-based morphometry--The methods. NeuroImage. 2000; 11:805–821. [PubMed: 10860804]

Ashburner J, Friston KJ. Unified segmentation. NeuroImage. 2005; 26:839–851. [PubMed: 15955494]

Benjamini Y, Hockberg Y. Controlling the false discovery rate: A practical and powerful approach to multiple testing. Journal of the Royal Statistical Society. 1995; 57:289–300.

Blair RJ. The emergence of psychopathy: Implications for the neuropsychological approach to developmental disorders. Cognition. 2006; 101:414–442. [PubMed: 16904094]

Blonigen DM, Hicks BM, Krueger RF, Patrick CJ, Iacono WG. Continuity and change in pscyhopathic traits as measured via normal-range personality: A longitudinalbiometric study. Journal of Abnormal Psychology. 2006; 115:85–95. [PubMed: 16492099]

Budhani S, Blair RJ. Response reversal and children with psychopathic tendencies: Success is a function of salience of contingency change. Journal of Child Psychology and Psychiatry. 2005; 46:972–981. [PubMed: 16109000]

Caldwell MF. Treatment-related changes in behavioral outcomes of psychopathy facets in adolescent offenders. Law and Human Behavior. 2011; 35:275–287. [PubMed: 20658262]

Caldwell MF, McCormick DJ, Umstead D, Van Rybroek GJ. Evidence of treatment progress and therapeutic outcomes among adolescents with psychopathic features. Criminal Justice and Behavior. 2007; 34:573–587.

Calhoun VD, Adali T, Pearlson GD, Pekar JJ. A method for making group inferences from functional MRI data using independent component analysis. Human brain mapping. 2001; 14:140–151. [PubMed: 11559959]

Calhoun VD, Maciejewski PK, Pearlson GD, Kiehl KA. Temporal lobe and "default" hemodynamic brain modes discriminate between schizophrenia and bipolar disorder. Human brain mapping. 2008; 29:1265–1275. [PubMed: 17894392]

Caprihan A, Abbott C, Yamamoto J, Pearlson G, Perrone-Bizzozero N, Sui J, Calhoun VD. Source-based morphometry analysis of group differences in fractional anisotropy in schizophrenia. Brain connectivity. 2011; 1:133–145. [PubMed: 22180852]

Coid J, Yang M, Ullrich S, Roberts A, Hare RD. Prevalence and correlates ofp sychopathic traits in the houshold population of Great Brittian. International journal of law and psychiatry. 2009; 32:65–73. [PubMed: 19243821]

Cope LM, Ermer E, Gaudet LM, Steele VR, Eckhardt AL, Arbabshirani MR, Caldwell MF, Calhoun VD, Kiehl KA. Abnormal brain structure in youth who commit homicide. NeuroImage: Clinical. 2014; 4:800–807. [PubMed: 24936430]

Dale AM, Fischl B, Sereno MI. Cortical surface-based analysis: I. Segmentation and surface reconstruction. NeuroImage. 1999; 9:179–194. [PubMed: 9931268]

Davidson RJ, Putnam KM, Larson CL. Dysfunction in the neural circuitry of emotion regulation--a possible prelude to violence. Science. 2000; 289:591–594. [PubMed: 10915615]

Dosenbach NUF, Nardos B, Cohen AL, Fair DA, Power JD, Church JA, Nelson SM, Wig GS, Vogel AC, Lessov-Schlaggar CN. Prediction of individual brain maturity using fMRI. Science. 2010; 329:1358–1361. [PubMed: 20829489]

Douglas, KS.; Webster, CD.; Hard, SD.; Eaves, D.; Ogloff, JRP. HCR-20 violence risk management companion guide. Simon Fraser University/University of South Florida; Vancouver, BC/Tampa, FL: 2002.

Ermer E, Cope LM, Nyalakanti PK, Calhoun V, Kiehl KA. Aberrant paralimbic gray matter in criminal psychopathy. Journal of abnormal psychology. 2012; 121:649–658. [PubMed: 22149911]

Ermer E, Cope LM, Nyalakanti PK, Calhoun VD, Kiehl KA. Aberrant paralimbic gray matter in incarcerated male adolescents with psychopathic traits. Journal of the American Academy of Child and Adolescent Psychiatry. 2013; 52:94–103. [PubMed: 23265637]

Fan, Y.; Rao, H.; Giannetta, J.; Hurt, H.; Wang, J.; Davatzikos, C.; Shen, D. Diagnosis of brain abnormality using both structural and functional MR images. Engineering in Medicine and Biology Society, 2006; EMBS'06. 28th Annual International Conference of the IEEE; IEEE; 2006. p. 1044-1047.

Farrington, DP. Family background in psychopathy. In: Patrick, C., editor. Handbook of Psychopathy. Guilford Press; New York: 2006. p. 229-250.

Forth, AE.; Kosson, DS.; Hare, RD. The Psychopath Checklist: Youth Version. Multi-Health Systems; Toronto: 2003.

Frick PJ, Cornell AH, Bodin SD, Dane HE, Barry CT, Loney BR. Callous-unemotional traits and developmental pathways to severe conduct problems. Developmental Psychology. 2003; 39:246–260. [PubMed: 12661884]

Habes I, Krall SC, Johnston SJ, Yuen KSL, Healy D, Goebel R, Sorger B, Linden DEJ. Pattern classification of valence in depression. NeuroImage: Clinical. 2013; 2:675–683. [PubMed: 24179819]

Hare, RD. Manual for the Hare Psychopathy Checklist-Revised. 2nd ed. Multi-Health Systems; Toronto, Canada: 2003.

Harenski CL, Harenski KA, Kiehl KA. Neural processing of moral violations among incarcerated adolescents with psychopathic traits. Developmental Cognitive Neuroscience. 2014

Harris GT, Rice ME, Quinsey VL. Violent recidivism of mentally disordered offenders the development of a statistical prediction instrument. Criminal Justice and Behavior. 1993; 20:315–335.

Hawkins, JD.; Herrenkohl, T.; Farrington, DP.; Brewer, D.; Catalano, RF.; Harachi, TW. A review of predictors of youth violence. 1998.

Hawkins JD, Herrenkohl TI, Farrington DP, Brewer D, Catalano RF, Harachi TW, Cothern L. Predictors of Youth Violence. Juvenile Justice Bulletin. 2000

Kiehl KA. A cognitive neuroscience perspective on psychopathy: Evidence for paralimbic system dysfunction. Psychiatry research. 2006; 142:107–128. [PubMed: 16712954]

King NS, Crawford S, Wenden FJ, Moss NE, Wade DT. The Rivermead post concussion symptoms questionnaire. Journal of Neurology. 1995; 242:587–592. [PubMed: 8551320]

Lee Z, Klaver JR, Hart SD, Moretti MM, Douglas KS. Short-term stability of psychopathic traits in adolescent offenders. Journal of Clinical Child and Adolescent Psychology. 2009; 38:595–605. [PubMed: 20183645]

Lockwood PL, Sebastian CL, McCrory EJ, Hyde ZH, Gu X, De Brito SA, Viding E. Association of callous traits with reduced neural response to others' pain in children with conduct problems. Current Biology. 2013; 23:901–905. [PubMed: 23643836]

Lynam DR, Caspi A, Moffitt TE, Loeber R, Stouthamer-Loeber M. Longitudinal evidence that psychopathy scores in early adolescence predict adult psychopathy. Journal of Abnormal Psychology. 2007; 116:155–165. [PubMed: 17324026]

Marhe R, van de Wetering BJ, Franken IH. Error-Related Brain Activity Predicts Cocaine Use After Treatment at 3-Month Follow-up. Biological psychiatry. 2013; 73:782–788. [PubMed: 23374638]

Marsh AA, Finger EC, Mitchell DGV, Reid ME, Sims C, Kosson DS, Towbin KE, Leibenluft E, Pine DS, Blair RJR. Reduced amygdala response to fearful expressions in children and adolescents with callous-unemotional traits and disruptive behavior disorders. American Journal of Psychiatry. 2008; 165:712–720. [PubMed: 18281412]

Melgani F, Bruzzone L. Classification of hyperspectral remote sensing images with support vector machines. Ieee Transactions on Geoscience and Remote Sensing. 2004; 42:1778–1790.

Moffitt TE. Adolescence-limited and life-course-persistent antisocial behavior: a developmental taxonomy. Psychological Review. 1993; 100:674. [PubMed: 8255953]

Monahan J. The clinical prediction of violent behavior. Crime & delinquency issues: A monograph series. 1981; 47:49.

Motzkin JC, Newman JP, Kiehl KA, Koenigs M. Reduced prefrontal connectivity in psychopathy. The Journal of Neuroscience. 2011; 31:17348–17357. [PubMed: 22131397]

Neumann CS, Hare RD. Psychopathic traits in a large community sample: links to violence, alcohol use, and intelligence. Journal of Consulting and Clinical Psychology. 2008; 76:893–899. [PubMed: 18837606]

Obradovic J, Pardini DA, Long JD, Loeber R. Measuring interpersonal callousness in boys from childhood to adolescence: an examination of longitudinal invariance and temporal stability. Journal of Clinical Child and Adolescent Psychiatry. 2007; 36:276–292.

Pardini DA, Raine A, Erickson K, Loeber R. Lower Amygdala Volume in Men is Associated with Childhood Aggression, Early Psychopathic Traits, and Future Violence. Biological Psychiatry. 2014; 75:73–80. [PubMed: 23647988]

Pariyadath V, Stein EA, Ross TJ. Machine learning classification of resting state functional connectivity predicts smoking status. Frontiers in human neuroscience. 2014:8. [PubMed: 24478674]

Raine A, Lencz T, Taylor K, Hellige JB, Bihrle S, Lacasse L, Lee M, Ishikawa S, Colletti P. Corpus callosum abnormalities in psychopathic antisocial individuals. Archives of General Psychiatry. 2003; 60:1134–1142. [PubMed: 14609889]

Rice ME, Harris GT. Cross-validation and extension of the violence risk appraisal guide for child molesters and rapists. Law and Human Behavior. 1997; 21:231–241. [PubMed: 9146103]

Rizk-Jackson A, Stoffers D, Sheldon S, Kuperman J, Dale A, Goldstein J, Corey-Bloom J, Poldrack RA, Aron AR. Evaluating imaging biomarkers for neurodegeneration in pre-symptomatic Huntington's disease using machine learning techniques. NeuroImage. 2011; 56:788–796. [PubMed: 20451620]

Rusconi E, Mitchener-Nissen T. Prospects of functional magnetic resonance imaging as lie detector. Frontiers in human neuroscience. 2013; 7:594. [PubMed: 24065912]

Ryan JJ, Lopez SJ, Werth TR. Development and preliminary validation of a Satz-Mogel short form of the WAIS-III in a sample with substance abuse disorders. International Journal of Neuroscience. 1999; 98:131–140. [PubMed: 10395365]

Sattler, JM.; Dumont, R. Assessment of Children: WISC-IV and WPPSI-II Supplement. Jerome M. Sattler; San Diego: 2004.

Savitz JB, Rauch SL, Drevets WC. Clinical application of brain imaging for the diagnosis of mood disorders: the current state of play. Molecular psychiatry. 2013; 18:528–539. [PubMed: 23546169]

Schnack HG, Nieuwenhuis M, van Haren NEM, Abramovic L, Scheewe TW, Brouwer RM, Pol HEH, Kahn RS. Can structural MRI aid in clinical classification? A machine learning study in two independent samples of patients with schizophrenia, bipolar disorder and healthy subjects. NeuroImage. 2014; 84:299–306. [PubMed: 24004694]

Silva, RF.; Castro, E.; Gupta, CN.; Cetin, M.; Arbabshirani, MR.; Potluru, VK.; Plis, SM.; Calhoun, VD. The tenth annual MLSP competition: Schizophrenia classification challenge. Machine Learning for Signal Processing (MLSP), 2014; IEEE International Workshop on; IEEE; 2014. p. 1-6.

Steele VR, Claus ED, Aharoni E, Vincent GM, Calhoun VD, Kiehl KA. Multimodal imaging measures predict rearrest. Frontiers in human neuroscience. 2015; 9:425. [PubMed: 26283947]

Steele VR, Fink BC, Maurer JM, Arbabshirani MR, Wilber CH, Jaffe AJ, Sidz A, Pearlson GD, Calhoun VD, Clark VP, Kiehl KA. Brain potentials measured during a Go/NoGo task predict completion of substance abuse treatment. Biological psychiatry. 2014; 76:75–83. [PubMed: 24238783]

Sui J, Adali T, Pearlson GD, Calhoun VD. An ICA-based method for the identification of optimal FMRI features and components using combined group-discriminative techniques. NeuroImage. 2009; 46:73–86. [PubMed: 19457398]

Sun D, van Erp TGM, Thompson PM, Bearden CE, Daley M, Kushan L, Hardt ME, Nuechterlein KH, Toga AW, Cannon TD. Elucidating a magnetic resonance imaging-based neuroanatomic biomarker for psychosis: classification analysis using probabilistic brain atlas and machine learning algorithms. Biological psychiatry. 2009; 66:1055–1060. [PubMed: 19729150]

Wechsler, D. Wechsler adult intelligence scale. Psychological Corporation; New York, NY: 1997.

Wechsler, D. Wechsler Intelligence Scale for Children - Fourth Edition: Technical and Interpretetive Manual. Psychological Corporation; San Antonio, TX: 2003.

Weygandt M, Blecker CR, Schäfer A, Hackmack K, Haynes J-D, Vaitl D, Stark R, Schienle A. fMRI pattern recognition in obsessive–compulsive disorder. NeuroImage. 2012a; 60:1186–1193. [PubMed: 22281674]

Weygandt M, Schaefer A, Schienle A, Haynes JD. Diagnosing different binge-eating disorders based on reward-related brain activation patterns. Human brain mapping. 2012b; 33:2135–2146. [PubMed: 22887826]

Xu L, Groth KM, Pearlson G, Schretlen DJ, Calhoun VD. Source-based morphometry: The use of independent component analysis to identify gray matter differences with application to schizophrenia. Human brain mapping. 2009; 30:711–724. [PubMed: 18266214]

Yang H, Liu J, Sui J, Pearlson GD, Calhoun VD. A hybrid machine learning method for fusing fMRI and genetic data: combining both improves classification of schizophrenia. Frontiers in human neuroscience. 2010a:4. [PubMed: 20198130]

Yang M, Wong SCP, Coid J. The efficacy of violence prediction: A meta-analytic comparison of nine risk assessment tools. Psychological bulletin. 2010b; 136:740–767. [PubMed: 20804235]

Yekutieli D, Benjamini Y. Resampling-based false discovery rate controlling multiple test procedures for correlated test statistics. Journal of Statistical Planning and Inference. 1997; 82:171–196.

Zhang, L.; Samaras, D.; Tomasi, D.; Volkow, ND.; Goldstein, RZ. Machine learning for clinical diagnosis from functional magnetic resonance imaging. Computer Vision and Pattern Recognition, 2005; IEEE Computer Society Conference on; IEEE; 2005. p. 1211-1217.CVPR 2005

Highlights

- SVM prediction models used neural correlates of a psychopathic traits
- SVM of VBM differentiated individuals with and without elevated psychopathic traits
- SVM of VBM differentiated individuals with psychopathic traits and healthy controls
- Additional personality measures could be used to aid in diagnosis and treatment

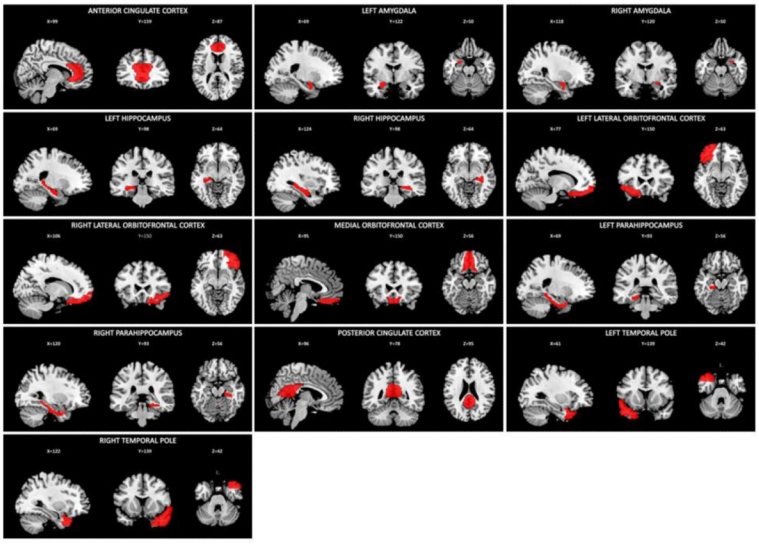

Figure 1.

Thirteen regions of interest masks used in the analyses are presented (ACC, bilateral Amygdala, bilateral Hippocampus, mOFC, bilateral OFC, bilateral Parahippocampus, PCC, and bilateral Temporal Pole).

Table 1

Support vector machine analyses grey matter volume and density predicting high vs low PCL: YV group

	All Volume ROIs	All Density ROIs	All Volume and Density ROIs	Age and IQ
Overall Classification Rate	67.13%	62.94%	69.23%	65.03%
Specificity	68.06%	69.44%	68.06%	76.39%
Sensitivity	66.20%	56.34%	70.42%	53.52%
Positive Predictive Value	67.14%	64.52%	68.49%	69.09%
Negative Predictive Value	67.12%	61.71%	70.00%	62.50%

Note: Four support vector machine (SVM) models predicting PCL: YV groups (30 and above vs 20 and below) were computed individually for measures of grey matter volume and density. Separate SVM models were calculated for all 13 ROIs (Models 1 & 2) as well as combining volume and density measures in the same SVM model (Model 3). Finally, age and IQ were included alone in a SVM (Model 4). Specificity is the measure of how well the model identified individuals in the low PCL: YV group and sensitivity is the measure of how well the model identified individuals in the high PCL: YV group. Positive predictive value represents the ratio of individuals who were identified to be in the low PCL: YV group to combined individuals identified correctly and incorrectly to be in the low PCL: YV group. Negative predictive value represents the ratio of individuals who were identified to be in the high PCL: YV group to combined individuals identified correctly and incorrectly to be in the high PCL: YV group. The C and σ identified for models 1 through 4 were: Model 1) C = 32.00, σ = 11.31; Model 2) C = 45,25, σ = 2.83; Model 3) C = 2.00, σ = 2.00; Model 4) C = 1.00, σ = 1.00. Permutation *p*-values related to the overall classification accuracy were calculated for each model: Model 1) $p = .017$; Model 2) $p = .098$; Model 3) $p = .024$; Model 4) $p = .045$.

Table 2

One-tailed t-tests comparing grey matter volume and density between groups

a.

Volume	*High vs Low PCL: YV groups*	*High PCL: YV group vs Healthy Controls*	*Low PCL: YV group vs Healthy Controls*
ACC	$t(141) = 0.30$, $p = .384$	$t(90) = 1.76$, $p = .049^{*}$	$t(91) = 2.30$, $p = .052^{\wedge}$
Left amygdala	$t(141) = 1.44$, $p = .198$	$t(90) = 1.83$, $p = .051^{\wedge}$	$t(91) = 1.02$, $p = .184$
Right amygdala	$t(141) = 1.44$, $p = .165$	$t(90) = 2.15$, $p = .037^{*}$	$t(91) = 1.36$, $p = .116$
Left hippocampus	$t(141) = 1.08$, $p = .262$	$t(90) = 2.08$, $p = .033^{*}$	$t(91) = 1.55$, $p = .102$
Right hippocampus	$t(141) = 0.99$, $p = .235$	$t(90) = 2.36$, $p = .026^{*}$	$t(91) = 1.94$, $p = .073^{\wedge}$
mOFC	$t(141) = 1.02$, $p = .250$	$t(90) = 2.15$, $p = .032^{*}$	$t(91) = 1.69$, $p = .102$
Left OFC	$t(141) = 0.83$, $p = .241$	$t(90) = 1.73$, $p = .047^{*}$	$t(91) = 1.49$, $p = .101$
Right OFC	$t(141) = 0.95$, $p = .222$	$t(90) = 2.49$, $p = .023^{*}$	$t(91) = 2.22$, $p = .046^{*}$
Left parahippocampus	$t(141) = 0.55$, $p = .314$	$t(90) = 3.00$, $p = .009^{**}$	$t(91) = 2.79$, $p = .020^{*}$
Right parahippocampus	$t(141) = 1.86$, $p = .074^{\wedge}$	$t(90) = 1.79$, $p = .051^{\wedge}$	$t(91) = 0.75$, $p = .248$
PCC	$t(141) = 2.09$, $p = .062^{\wedge}$	$t(90) = 1.32$, $p = .095^{\wedge}$	$t(91) = 0.01$, $p = .494$
Left temporal pole	$t(141) = 2.34$, $p = .065^{\wedge}$	$t(90) = 4.34$, $p < .013^{*}$	$t(91) = 3.02$, $p = .013^{*}$
Right temporal pole	$t(141) = 2.96$, $p = .026^{*}$	$t(90) = 3.46$, $p < .007^{**}$	$t(91) = 1.67$, $p = .091^{\wedge}$

b.

Density	*High vs Low PCL: YV groups*	*High PCL: YV group vs Healthy Controls*	*Low PCL: YV group vs Healthy Controls*
ACC	$t(141) = 0.47$, $p = .413$	$t(90) = 3.33$, $p < .013^{*}$	$t(91) = 3.35$, $p < .013^{*}$
Left amygdala	$t(141) = 0.68$, $p = .542$	$t(90) = 2.75$, $p = .006^{**}$	$t(91) = 3.35$, $p < .007^{**}$
Right amygdala	$t(141) = 0.88$, $p = .618$	$t(90) = 2.94$, $p = .003^{**}$	$t(91) = 2.51$, $p = .010^{*}$
Left hippocampus	$t(141) = 0.16$, $p = .476$	$t(90) = 2.20$, $p = .020^{*}$	$t(91) = 1.85$, $p = .044^{*}$
Right hippocampus	$t(141) = 0.57$, $p = .463$	$t(90) = 1.63$, $p = .053^{\wedge}$	$t(91) = 1.22$, $p = .112$
mOFC	$t(141) = 0.49$, $p = .387$	$t(90) = 4.12$, $p < .007^{**}$	$t(91) = 4.35$, $p < .004^{**}$
Left OFC	$t(141) = 0.60$, $p = .509$	$t(90) = 4.96$, $p < .004^{**}$	$t(91) = 4.81$, $p < .003^{*}$
Right OFC	$t(141) = 0.16$, $p = .439$	$t(90) = 2.20$, $p = .018^{*}$	$t(91) = 1.85$, $p = .040^{*}$
Left parahippocampus	$t(141) = 0.73$, $p = .606$	$t(90) = 4.89$, $p < .003^{**}$	$t(91) = 5.38$, $p < .003^{**}$
Right parahippocampus	$t(141) = 0.54$, $p = .425$	$t(90) = 4.17$, $p < .003^{**}$	$t(91) = 4.21$, $p < .002^{**}$
PCC	$t(141) = 1.03$, $p = .663$	$t(90) = 1.91$, $p = .033^{*}$	$t(91) = 1.37$, $p = .095^{\wedge}$
Left temporal pole	$t(141) = 1.30$, $p = .637$	$t(90) = 6.27$, $p < .002^{**}$	$t(91) = 5.70$, $p < .002^{**}$
Right temporal pole	$t(141) = 1.44$, $p = .988$	$t(90) = 5.73$, $p < .002^{**}$	$t(91) = 4.98$, $p < .002^{**}$

Note. One-tailed independent samples *t*-tests between groups are presented for each ROI. Tests of differences in volume are reported in table 4a and tests of differences in density are reported in table 4b. All differences between high and low PCL: YV groups are due to reduced grey matter volume or density in the high PCL: YV group, compared to the low PCL: YV group. All differences in comparisons with healthy controls are due

to reduced grey matter volume or density in the PCL: YV group, compared to healthy controls. All *p*-values have been corrected with false-discovery rate correction for multiple comparisons (Benjamini and Hockberg, 1995; Yekutieli and Benjamini, 1997).

$^{\wedge}p < .10$

$^{*}p < .05;$

$^{**}p < .01.$

Table 3

Support vector machine analyses grey matter volume and density predicting high PCL: YV group vs healthy controls

	All Volume ROIs	All Density ROIs	All Volume and Density ROIs	Age and IQ
Overall Classification Rate	70.65%	82.61%	78.26%	83.70%
Specificity	73.24%	83.10%	77.46%	85.92%
Sensitivity	61.90%	80.95%	80.95%	76.19%
Positive Predictive Value	40.62%	58.62%	51.52%	61.54%
Negative Predictive Value	86.67%	93.65%	93.22%	92.42%

Note: Four support vector machine (SVM) models predicting high PCL: YV group (30 and above) and healthy controls were computed individually for measures of grey matter volume and density. Separate SVM models were calculated for all 13 ROIs (Models 1 & 2) as well as combining volume and density measures in the same SVM model (Models 3). Finally, age and IQ were included alone in a SVM (Model 4). Specificity is the measure of how well the model identified individuals in the high PCL: YV group and sensitivity is the measure of how well the model identified healthy control individuals. Positive predictive value represents the ratio of individuals who were identified to be in the high PCL: YV group to combined individuals identified correctly and incorrectly to be in the high PCL: YV group. Negative predictive value represents the ratio of individuals who were identified to be healthy controls to combined individuals identified correctly and incorrectly to be healthy controls. The C and σ identified for models 1 through 4 were: Model 1) C = 64.00, σ = 11.31; Model 2) C = 64.00, σ = 8.00; Model 3) C = 2.83, σ = 11.31; Model 4) C = 0.25, σ = 0.77. Permutation *p*-values related to the overall classification accuracy were calculated for each model: Model 1) $p = .213$; Model 2) $p = .007$; Model 3) $p = .042$; Model 4) $p = .003$.

Table 4

Support vector machine analyses grey matter volume and density predicting low PCL: YV group vs healthy controls

	All Volume ROIs	All Density ROIs	All Volume and Density ROIs	Age and IQ
Overall Classification Rate	76.34%	80.65%	79.57%	83.87%
Specificity	83.33%	83.33%	80.56%	83.33%
Sensitivity	52.38%	71.43%	76.19%	85.71%
Positive Predictive Value	47.83%	55.56%	53.33%	60.00%
Negative Predictive Value	85.71%	90.91%	92.06%	95.24%

Note: Four support vector machine (SVM) models predicting low PCL: YV group (20 and below) and healthy controls were computed individually for measures of grey matter volume and density. Separate SVM models were calculated for all 13 ROIs (Models 1 & 2) as well as combining volume and density measures in the same SVM model (Model 3). Finally, age and IQ were included alone in a SVM (Model 4). Specificity is the measure of how well the model identified individuals in the low PCL: YV group and sensitivity is the measure of how well the model identified healthy control individuals. Positive predictive value represents the ratio of individuals who were identified to be in the low PCL: YV group to combined individuals identified correctly and incorrectly to be in the low PCL: YV group. Negative predictive value represents the ratio of individuals who were identified to be healthy controls to combined individuals identified correctly and incorrectly to be healthy controls. The C and σ identified for models 1 through 4 were: Model 1) C = 32.00, σ = 4.00; Model 2) C = 64.00, σ = 8.00; Model 3) C = 22.63, σ = 16.00; Model 4) C = 5.66, σ = 5.66. Permutation *p*-values related to the overall classification accuracy were calculated for each model: Model 1) $p = .055$; Model 2) $p = .011$; Model 3) $p = .021$; Model 4) $p = .004$.